Chinese Journal of Polar Science, Vol. 18, No. 1, 36-46, June 2007

# Sea ice thickness measurement in spring season in Bothnian Bay using an electromagnetic induction instrument

Guo Jingxue(郭井学) and Sun Bo(孙　波)
*Polar Research Institute of China, Shanghai 200136, China*

Received May 10, 2007

**Abstract** As an important component of the cryosphere, sea ice is very sensitive to the climate change. The study of the sea ice physics needs accurate sea ice thickness. This paper presents an electromagnetic-induction (EM) technique which can be used to measure the sea ice thickness distribution efficiently, and the successful application in Bothnian Bay. Based on the electromagnetic field theory and the electrical properties of sea ice and seawater, EM technique can detect the distance between the instrument and the ice/water interface accurately, than the sea ice thickness is obtained. Contrastive analysis of the apparent conductivity data obtained by EM and the value of drill-hole at same positions allows a construction of a transformable formula of the apparent conductivity to sea ice thickness. The verification of the sea ice thickness calculated by this formula indicates that EM technique is able to get reliable sea ice thickness with average relative error of only 12%. The statistic of all ice thickness profiles shows that the level ice distribution in Bothnian Bay was 0.4 – 0.6 m.
**Key words** Electromagnetic-induction, Sea ice, Thickness, Bothnian Bay.

## 1 Introduction

Sea ice is a component of cryosphere in the earth climate system. It is very sensitive to climatic change. The thickness and change of sea ice has particularly significant effect on the coupling of atmosphere – sea-ice – ocean and directly determines the course and speed of energy and substance exchange between sea and air[1,2]. The ice thickness is characterized by the sea ice dynamics and thermodynamics via various processes of drift, deformation, freezing and melting. Therefore, the research on physical process of sea ice needs precisely accurate thickness data of sea ice[3,4]. The effective technology of detecting ice thickness includes satellite remote sensing, and using underwater sonar, upward looking radar, electromagnetic-induction technique and hole-drilling. The most potential method of satellite remote sensing is to measure the height of freeboard firstly and then calculate the thickness of sea ice with the law of Archimedes. But the sea level derived from GPS geoid surface data may be with some error, which consequently lim its the accuracy of freeboard height measured with satellite[5-7]; underwater sonar can get depth of the draft which then is converted into the thickness of sea ice. The accuracy is limited by the position of underwater transducer and the effect of the changes of water temperature, tide and pressure change[8]. Radar detection may easily have major error at the place where the sea ice is inhomogeneous[9]. Drilling is the most immediate and reliable method, but it can't meet the demand of large-scale observation due to its low efficiency. Detection of sea ice thickness by electromagnetic induction (EM) has been introduced to the research of sea ice gradually from the 1990s. Based on the difference between the electrical properties of sea ice and that of seawater, it can be used to determine the thickness of sea ice quickly without contacting and has high precision and reliability. As flexible in use, it can be used to detect the thickness of sea ice directly above from the ice surface and by means of shipborne and airborne. The observations can directly correct and verify the observed data of satellite remote sensing and provide valuable information for calculation of sea ice numerical model on different scale in the research of climatic change. Due to its rapidness and flexibility, this technology has attracted attention in the world and been taken on a booming trend in recent years. It is considered as the observation technology with the biggest development potential[10].

Bothnian Bay is located at the north of Baltic Sea, between Finland and Sweden, 650 km long, 250 km at the widest place, with an area of 117000 km$^2$ and about 5 months of sea ice season per year. To ensure safe winter shipping and learn the effect of sea ice on the climate in this region, in the past 10-odd years, sea ice in this sea area was monitored and researched on different scale. Finnish Institute of Marine Research (FIMR) and Helsinki University of Technology (HUT) has undertaken the project of Multipolarization SAR for Operational Sea Ice Monitoring (POL-ICE), which was sponsored by Finnish Funding Agency for Technology and Innovation (TEKES) and organized an associated sea ice survey. The field survey of 2007 was carried out on March 5-16 at Bothnian Bay Research Station at Hailuoto Island. Polar Research Institute of China (PRIC), as a long-term copartner of FIMR, took part in this field observation. Besides, there were also survey personnel from Germany, Canada and Japan. The main tasks of this survey was to review sea ice monitoring requirements, collect observational data of ice surface on different scale and develop sea ice monitoring technology systematically. In the survey, our assignment was to detect the ice thickness directly on the ice surface of Bothnian Bay with EM technique as the foundation for further research.

This paper focuses on discussion on the characteristics of detection of sea ice thickness with EM at Bothnian Bay and gives the sea ice thickness profiles and sea ice thickness distribution.

## 2 Instruments and theory

The main equipment adopted is EM31 made by Geonics of Canada. It is a portable, small-offset loop-loop steady-state induction device. The spacing between the coplanar transmitter and receiver antenna coils is 3.66 m and the operating frequency is 9.8 kHz. The instrument can be operated with coils either vertically or horizontally aligned, corresponding to the horizontal or vertical magnetic dipole (HDM or VDM) mode, respectively, as shown in Fig. 1, with depth penetration of 3 m and 6 m respectively[11]. The instrument measures the quadrature component response of secondary magnetic field. The quadrature response is automatically transformed to an apparent conductivity in mS/m. The sampling frequency of this instrument is 1 s. The weight of this instrument is about 11Kg. For operation, it should only be hanged at the operator's shoulders and measurement of sea ice thickness can be completed during walking

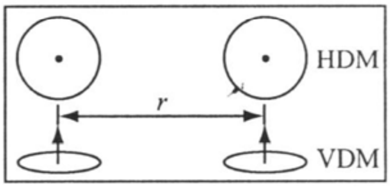


Fig 1 Sketch showing horizontal dipole mode (HDM) and vertical dipole model (VDM).

EM measurements of sea ice thickness rely on the large contrast in electrical conductivity of sea ice and that of seawater, as the electrical conductivity of seawater is far greater than the sea ice, consequently the conductivity of the sea ice is negligible[12]. Therefore, a quasi-static low-frequency EM field generated by the transmitter coil of the EM instrument will induce eddy currents mainly in the seawater below the ice. It, in turn, will result in a secondary field which is sensed by a receiver coil. The secondary-to-primary field ratio can be expressed in terms of an apparent conductivity $\sigma_a$:

$$\sigma_a = \frac{4}{\omega \mu_0 r^2} \left| \frac{H_S}{H_P} \right| \quad (1)$$

Here, $H_P$ is primary magnetic field intensity, $H_S$ is the secondary magnetic field intensity, $\omega$ is the angular frequency ( = $2\pi f$); $\mu_0$ is the magnetic permeability of free space; $r$ is the spacing between transmitter coil and receiver coil.

The apparent conductivity is a measure of integrated electrical conductivity of the half-space underneath the instrument. Because the sea ice electrical conductivity is so small that it can be ignored, the value of apparent conductivity $\sigma_a$ only depends on the distance $T_I$ from the instrument to the ice-water interface and the value of seawater electrical conductivity. If the seawater electrical conductivity is considered to be constant, $\sigma_a$ is just the function of $T_I$, the distance from the instrument to the ice-water interface. Theoretically, it is a negative exponential relation between apparent conductivity $\sigma_a$ and height $T_I$[10]. Therefore, via accurate measurement of apparent conductivity $\sigma_a$, the height $T_I$ from instrument to ice-water interface can be obtained by converting the apparent conductivity $\sigma_a$ provided that seawater electrical conductivity is given. When measurement directly on ice surface, i. e., EM31 is put on the ice, $T_I$ is the thickness of sea ice. During the measuring process, for the convenience of operation, the observer needs to carry the instrument up. This will bring up a space between the EM31 instrument and the ice surface and consequently affect the observation results. For this reason, Geonics designed EM31 for carrying and calibrate default height of instrument to be 1.1m. In this way, it can be considered that observation with instrument carried up as direct observation on the ice surface and consequently the work efficiency greatly increased. Most of the sea ice is covered by snow, while the electrical conductivities of both snow and sea ice are very small and neglectable relative to seawater electrical conductivity, so this method can't differentiate snow and ice and the measured value $T_I$ of sea ice thickness is the thickness of snow and ice.

## 3 Work area and methods

The measurements were performed as part of geophysical expedition to Bothnian Bay, during March 2007 (Fig. 2). Profiles observed by EM31 are the P1-P4 lines. The main working places are about 4km to the land (Hailuoto). The sea ice in this area is mostly level ice with little deformed ice ridge. The ice surface is covered with snow of 2-15 cm.

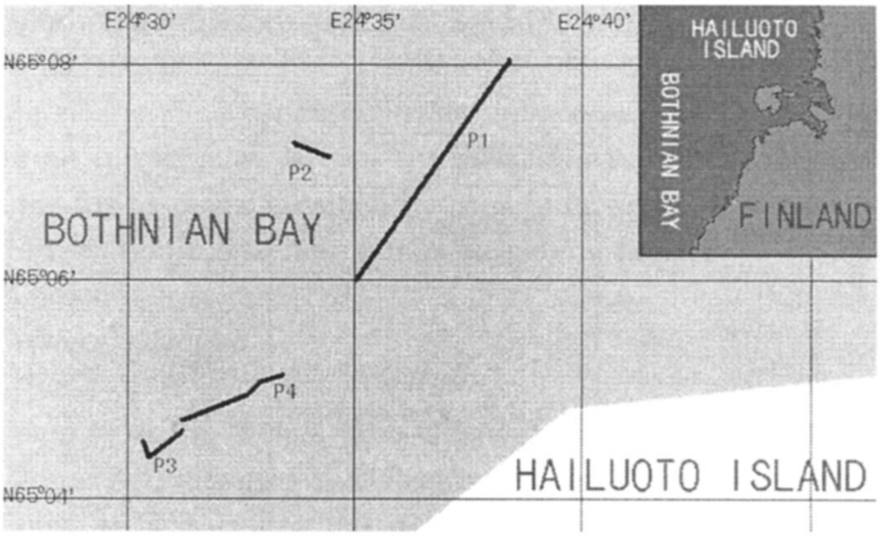


Fig. 2 Map of the expedition region in Bothnian Bay showing the location of sea ice thickness profiles measured by electromagnetic method

Measurement of sea ice thickness with EM31 together with drilling is one of the important contents of this survey. To achieve a better resolution, HMD mode was adopted to achieve EM31 measurement[13]. First of all, typical positions were selected in the area of level ice and deformed ice to complete measuring of 86 holes drilled. EM31 is adopted at every hole position to observe the apparent conductivity $\sigma_a$. Through these measurements, the relation between sea ice thickness and apparent conductivity at Bothnian Bay is developed ($\sigma_a / T_I$). Then 120 holes drilled measurements for sea ice thickness are completed in a larger scale, EM31 is adopted at the same position to observe apparent conductivity to develop verification of $\sigma_a / T_I$ relation. Finally, with the high efficiency advantage of EM31, 4 profiles at length from 510 m to 4500 m in different areas are completed (P1, P2, P3, and P4, Fig. 2).

## 4 Model calculation and data analysis

### *4.1 Forward modeling and data fitting*

The purpose of computational model response is to study the relation between apparent conductivity $\sigma_a$ and sea ice thickness $T_I$. Wait (1982)[14] gave the calculation expression of stratified model response. Kaufman and Keller (1983)[15] verified the model program via tabular calculation with stratified model comparison. By early this century, stratified model had already been able to simulate ice thickness relatively under different conditions accurately. What is used here is the model optimized by Christian Haas in the last few years through complete resolution formula and digital filtering approach.

According to the practical situation of sea ice in Bothnian Bay, two layers model was used to study the forward response of EM31. These two layers are the sea ice with limited thickness and the seawater with infinite thickness (Fig. 3). The sea ice is assumed to have a conductivity of zero, the seawater conductivity is taken from field measurement, and the average measuring result is 200 mS/m. Fig. 4 shows the relation between apparent conductivity and ice thickness under HMD mode. The dashed is the forward curve of two-layer model and the solid line is the curve obtained by fitting the data on 86 holes. The fitting formula is

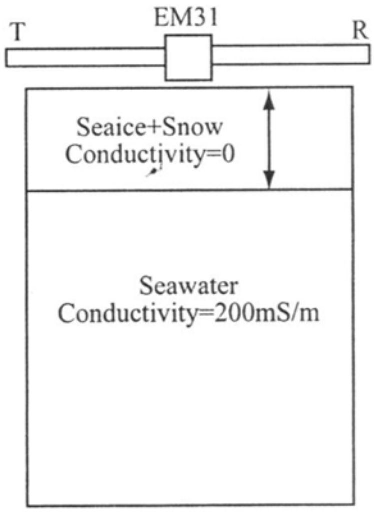


Fig. 3 Sketch of the two layers model

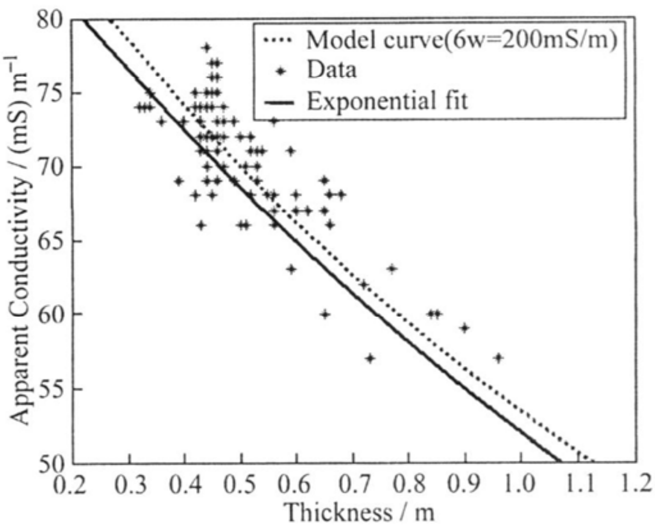


Fig. 4 The relationship between the apparent conductivity and the drill-hole value

$$\sigma_a = a e^{(bT_I)} \quad (2)$$

$a = 90.547$; $b = -0.5335$. Drill and observation of apparent conductivity with EM31 at the same position are required to be completed on sea ice at sites of different thicknesses to make the data typical, accurately and reliably. During the course of field observation, the observation is completed on sea ice at different thicknesses based on the physical conditions as far as possible. It is shown in Fig. 4 that the ice thickness at the observation area varies from 0.3m to 1m, thus the value of apparent conductivity under different ice thicknesses can be obtained and EM31 observation characteristics can be embodied systematically. As a result, the data fitting and the conversion from apparent conductivity to sea ice thickness to be described later will be more accurate and reliable.

Fig 4 shows the measurement relation between apparent conductivity and ice thickness. There is deviation between the fitting curve based on observed data and the curve of theoretical model. There are many causes for the deviation and it can't be explained with any single factor. One of the main factors is the effect brought by the seawater electrical conductivity. We measured the seawater electrical conductivity and the average value obtained is 200mS/m. The model curve is obtained through calculation based on this average value. The main advantage with EM is wide-range detection with its high-efficiency. The variation of seawater electrical conductivity in practice is hard to be avoided. In addition, the content of brine in seawater is also a factor influencing EM31 measuring result. All these show that the fitting curve obtained by combining apparent conductivity data and drill data from field observation meets the practical situation better.

### 4.2 $\sigma_a$-to-$T_I$ transformation

It can be learnt from Fig 4 that there is deviation of the practical fitting curve from the theoretical model curve, indicating that during the actual measurement the conversion between $\sigma_a$ and $T_I$ has to be based on the approximate experience equation[13]. This method has been widely used by experts throughout the world and can give reliable results. As mentioned above, there is a negative exponential relation between $\sigma_a$ and $T_I$. Therefore, from the equation (2) of observed data fitting, the calculation equation of ice thickness with apparent conductivity can be derived as follows:

$$T_I = -\frac{1}{0.53351}\ln(\sigma_a/90.547) \qquad (3)$$

Based on this relation, EM31 can achieve large-scale observation of sea ice thickness.

### 4.3 Validation by drill

To further verify the accuracy of sea ice thickness calculation of equation (3), different places were choose to complete drilling and EM31 observation again. Observations at 120 points were done. Via calculation by equation (3), apparent conductivity observed by EM31 were converted into sea ice thickness and compared with the thickness data measured by drilling (Fig 5). In order to evaluate the detection results with EM better and more comprehensively, deformed ice areas for observation besides level ice areas. In all measuring points, those of thickness less than 50cm accounts for about 50%, and 50cm to 1m for about 36%, over 1m for about 14%.

To analyze the error of sea ice thickness detected with EM quantitatively, the average relative error ($Rd$) of sea ice thickness detected by EM31 relative to drill was calculated as

$$Rd = \frac{\sum_{i=1}^{n}(|X_i - Y_i|/Y_i) \times 100\%}{n} \qquad (4)$$

Here, $X_i$ is the sea ice thickness from EM31; $Y_i$ is the sea ice thickness from drill; n is 120, the number of points.

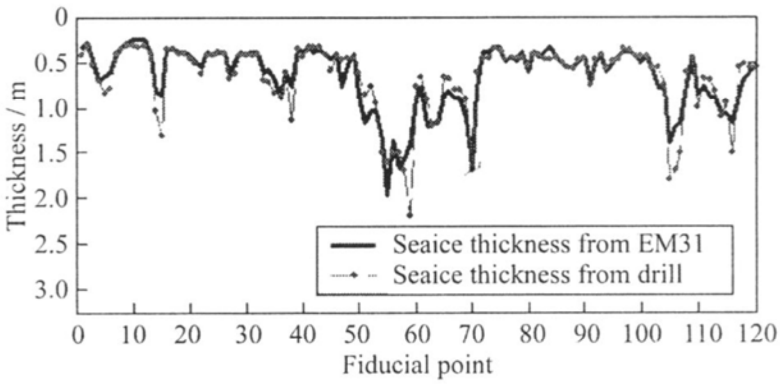


Fig 5 Comparison of sea ice thickness measured by EM31 and drill

Via calculation by equation (4), the average relative error of sea ice thickness from EM31 relative to that from drill is about 12%, indicating that the accuracy of sea ice thickness detection with EM31 is really high. It can be seen from Fig 5 that at the measuring points with fierce fluctuation of sea ice the fitting is low, because EM31 measuring results are not of single points, but calculated values of average depth under the coverage area. For different modes of coil, the diameter of coverage area is 1.3 to 3.8 times of the height from instrument to water surface[12, 16]. Therefore, when the sea ice thickness at observing point varies fiercely, the measuring error of EM31 will be relatively large.

## 5 Observation results and analysis

### 5.1 *Profiles of sea ice thickness*

Apparent conductivity for 4 long-distance profiles were made (Fig 2) with operators walking on ice surface and EM31 on the shoulder, and apparent conductivity transformed into thickness then. The sea ice thicknesses in a certain range are obtained and thus the efficiency of sea ice thickness detection on ice surface is increased greatly. Fig 6 shows the sea ice thickness of P1, P2, P3 and P4 profile respectively. The dot-dash line in the figure is the sea ice thickness transformed from apparent conductivity. Because the observation was carried out during walking, there is some disturbance in sea ice thickness calculated with raw data. Running mean (10 points) was adopted to eliminate the noise in the data (solid line in Fig 6) to observe the trend of sea ice thickness variation.

**P1:** this profile is the longest one among the 4 profiles, with a total length of 4500 m. The area where P1 located is a deep water area (water depth over 10 m) far from the bank in level ice areas. It can be seen from Fig 6 that the sea ice has relative spatial variation of ice thickness, which ranges from 40 cm to 60 cm; the sea ice thickness at 3500 m to 4000 m far has relatively larger variation, which may be the small-scale local variation generated by ice layer overlapping. Relative to the length of the entire profile, the variation of ice thickness is not very fierce but slow thickening and thinning.

**P2:** the total length of this profile is about 510 m, also located at the deep water area (water depth over 10 m) far from the bank. The part from 0 to 300 m of this profile is in a deformed ice area, including large ice ridge badly deformed by pressure. The average height of ice ridge over the level ice is about 50 cm. The part after 300 m of the profile is in a level ice area It can be seen that the variation in thickness of level ice ( about 40 cm) is not obvious, while the variation in thickness in ice ridge area is fierce, with maximum thickness exceeding 1. 5 m.

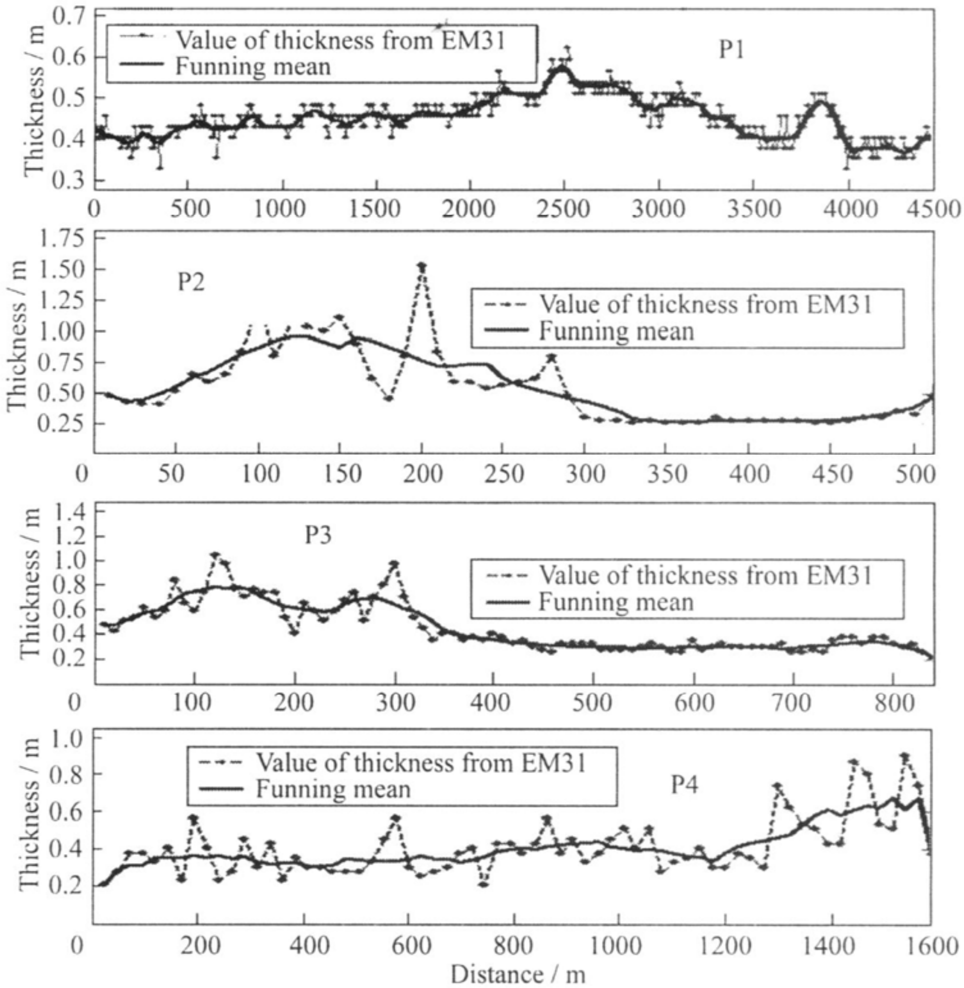


Fig 6 The profiles of sea ice thickness measured by electromagnetic-induction

**P3**: the total length of this profile is about 840 m with conditions similar to P2 The first 300 m is deformed ice area and the rest is level ice It must be explained that at the level ice parts, because a wide crack was met during observation and couldn't be spanned, the direction was changed and a turning curve section was formed

**P4**: this profile is the most complicated one, with length of about 1600 m. In Fig 2, it can be seen that P4 profile is not straight, because an area with both deformed ice and level ice was selected The ice ridge on this profile is not so badly deformed as that on P2, but the quantity of ice ridges is far more than that on P2 profile In the Fig 6, it can be seen that the variation of ice thickness measured by EM 31 is large, because the observer stood on the ice ridges to measure at a distance The running means indicates that the sea ice thickness is increasing

## *5. 2 Statistical analysis on ice thickness*

Fig 7 gives the frequency histograms for the sea ice thickness of the four profiles and the overall frequency histogram of ice thickness for the four profiles, as well as a normal fitted line The maximum normal fitting values of the four profiles are at the ice thickness of

0.45 m, 0.51 m, 0.46 m and 0.40 m respectively, while the maximum normal fitting value of the overall ice thickness is 0.47 m. In the histogram, it can also be seen that level ice accounts for the significant majority of sea ice in Bothnian Bay, the ice thickness ranges from 0.4 m to 0.6 m. The thickness of a small part of sea ice is greater than 0.6m and some ice ridges have thickness over 1 m.

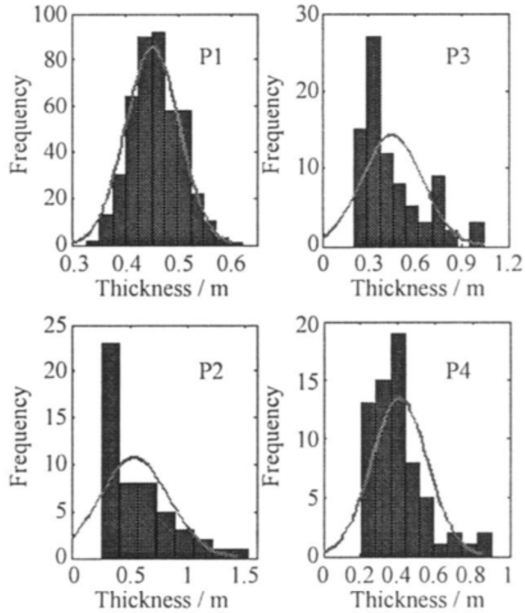


Fig 7a Statistics of sea ice thickness for each profile

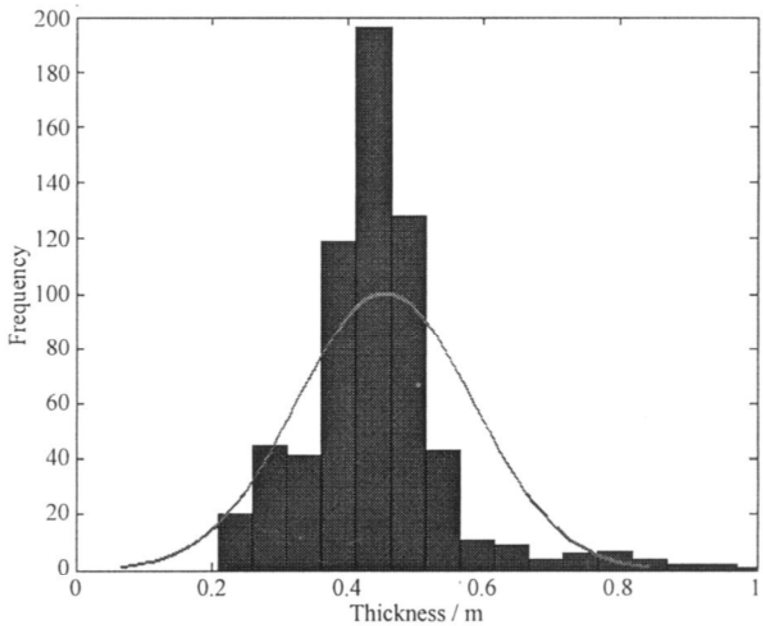


Fig 7b Statistics of sea ice thickness for all profile

Fig 7 Statistics of sea ice thickness of profiles measured by ground-based electromagnetic-induction

## 6 Conclusion and discussion

The electromagnetic induction technology is used in detection of sea ice thickness in Bothnian Bay successfully.

(1) Based on comparative analysis on 86 groups of apparent conductivity data observed with EM and drill data, the conversion relation between apparent conductivity and

sea ice thickness is obtained, and consequently the sea ice thickness can be figured out with the apparent conductivity directly read from EM instrument, providing calculation basis for accurate detection of sea ice thickness in Bothnian Bay with EM.

(2) The results of quality analysis on sea ice thickness detected with EM show that the technology has very high accuracy and the average relative error is only 12%, which meets the need for large-scale sea ice thickness detection.

(3) The statistical analysis on the results of sea ice thickness detection from 4 profiles shows that the thickness of level ice in Bothnian Bay in spring of 2007 ranges from 0.4m to 0.6m. The thickness of hummocked ice is over 1.5m at some points.

This article mainly discusses the application of EM technology in detection of sea ice thickness on ice. In practice, this technology can be extended to shipborne and airborne so that a larger range of sea ice thickness detection can be realized to provide basis for observation data of satellite remote sensing and provide valuable information for large-scale sea ice digital model in the research of climatic change.

As in current researches, there is still some error in sea ice thickness measurement with EM in the area with rich deformed ice. With changing the parameters of the instrument (such as working frequency or coil spacing) or improving the ice thickness inversion calculation method the errors of detection under special ice conditions will be reduced. This is one of future research contents.

**Acknowledgements** This work was supported by National Natural Science Foundation of China (Grant No. 40476005 and 40233032), the Ministry of Science and Technology, China (Grant No. 2005DIB3J114) and '863 Project' (Grant No. 2006AA04Z206 and 2006AA09Z152).

## References

[1] Dickson B (1999): All change in the Arctic Ocean. Nature, 397: 389-391.

[2] Marcel N (2003): Observations of superimposed ice formation at melt-onset on fast ice on Kongsfjorden, Svalbard. Physics and Chemistry of the Earth, 28: 1241-1248.

[3] Xie SM, Bao CL, Hao CJ (1995): Interaction Between sea ice of the Antarctic and Arctic. Chinese Science Bulletin, 40(7): 632–635 (in Chinese).

[4] Wu HD, Bai S, Zhang ZH (1998): Numerical simulation for dynamical processes of sea ice. Acta Oceanologica Sinica, 20(2): 1–13 (in Chinese).

[5] James BA *et al.* (2005): Geoscience Laser Altimeter System (GLAS) on the ICESat Mission: On-orbit measurement performance. Geophysical Research Letters, 2005, 32, L21S02, doi: 10.1029/2005GL024028.

[6] Johannesen OM, Shalina EV, Miles MW (1999): Satellite evidence for an Arctic sea ice cover in transform. Science, 286: 1937-1939.

[7] Guo FL, Zhao RY, Wang WB (2000): Application of passive Microwave Remote sensing to Sea Ice Thickness Measurement. Journal of Remote Sensing, 4(2): 112–117 (in Chinese).

[8] Paul GF, Pete S, Andrew SB (2003): Autonomous underwater vehicles: future platforms for fisheries acoustics. Ices Journal of Marine Science, 60: 684-691.

[9] Sun B, Wen JH, He MB *et al.* (2002): Sea ice thickness measurements and its underside morphology analysis using radar penetration in the Arctic Ocean. Science in China (Series D), 2002, 32(11): 951-958.

[10] Haas C (1998): Evaluation of ship-based electromagnetic-inductive thickness measurements of summer

sea ice in the Bellingshausen and Amundsen seas. Antarctica. Cold Regions Science and Technology, 27: 1-16.
[11] James ER *et al.* (2003): Shipborne electromagnetic measurements of Antarctic sea-ice thickness. Geophysics, 68(5): 1537-1546.
[12] Kovacs A *et al.* (1995): The footprint/altitude ratio for helicopter electromagnetic sounding of sea-ice thickness. Comparison of theoretical and field estimates. Geophysics, 60: 374-380.
[13] Kunio S *et al.* (2006): Ship-borne electromagnetic induction sounding of sea ice thickness in the Arctic during summer 2003. Polar Meteorol. Glaciol., 20: 53-61.
[14] Wait JR (1982): Geo-electromagnetism. Academic Press.
[15] Kaufman AA and Keller GV (1983): Frequency and transient soundings. Elsevier Science Publ. Co., Inc.
[16] Liu G, Becker A (1990): Two-dimensional mapping of sea ice keels with airborne electromagnetics. Geophysics, 55: 239-248.